

Quarkonium measurements via the di-muon decay channel in p+p and Au+Au collisions with the STAR experiment

Takahito Todoroki (for the STAR collaboration)

Brookhaven National Laboratory, Upton, New York 11973, USA

E-mail: todoroki@bnl.gov

Abstract. We present the first J/ψ and Υ measurements in the di-muon decay channel at mid-rapidity at RHIC using the newly installed Muon Telescope Detector. In p+p collisions at $\sqrt{s} = 500$ GeV, inclusive J/ψ cross section can be described by CGC+NRQCD and NLO NRQCD model calculations for $0 < p_T < 20$ GeV/ c . In Au+Au collisions at $\sqrt{s_{NN}} = 200$ GeV, we observe (i) clear J/ψ suppression indicating dissociation; (ii) J/ψ R_{AA} can be qualitatively described by transport models including dissociation and regeneration with a tension at high p_T ; and (iii) hint of less melting of $\Upsilon(2S + 3S)$ relative to $\Upsilon(1S)$ at RHIC compared to that at LHC.

1. Introduction

Quarkonia are an essential probe to study the properties of the Quark Gluon Plasma (QGP). The suppression of J/ψ due to color-screening effects in the medium was initially proposed as a direct evidence of the QGP formation [1]. However, the interpretation of the J/ψ suppression is still a challenge due to the contributions from the regenerated J/ψ by the recombination of $c\bar{c}$ pairs in the medium and the cold nuclear matter effects. Therefore it is important to have more precise J/ψ measurements over a broad kinematic range and even cleaner Υ state measurements. The latter do not suffer from the regeneration contribution due to the much smaller $b\bar{b}$ pair cross section, i.e. $\sigma_{b\bar{b}} \sim 2 \mu\text{b}$ [2] while $\sigma_{c\bar{c}} \sim 800 \mu\text{b}$ [3] at top RHIC energy. The newly installed Muon Telescope Detector (MTD), which provides both the di-muon trigger and the muon identification capability at mid-rapidity, opens the door to measuring quarkonia via the di-muon decay channel at STAR. Compared to the di-electron decay channel, the di-muon decay channel suffers much less from bremsstrahlung and thus provides much better invariant mass resolution to separate different Υ states. Using the MTD di-muon trigger, the STAR experiment recorded data corresponding to an integrated luminosity of 28.3 pb^{-1} in p+p collisions at $\sqrt{s} = 500$ GeV in the RHIC 2013 run, and 14.2 nb^{-1} in Au+Au collisions at $\sqrt{s_{NN}} = 200$ GeV in the RHIC 2014 run. In these proceedings, we report (1) the measurements of J/ψ production in p+p collisions at $\sqrt{s} = 500$ GeV; and (2) the measurements of the nuclear modification factor (R_{AA}) for J/ψ and the production of different Υ states in Au+Au collisions at $\sqrt{s_{NN}} = 200$ GeV.

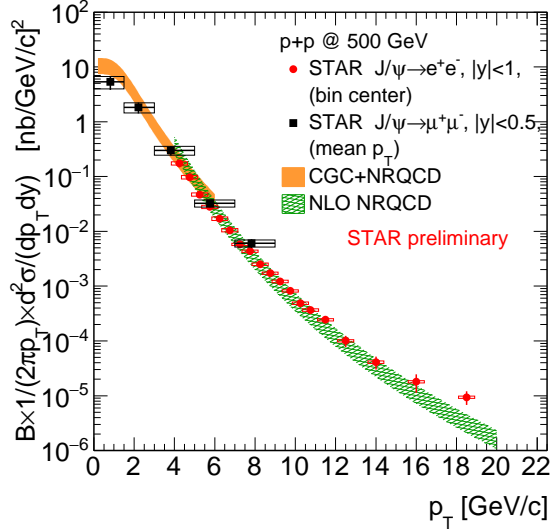


Figure 1. J/ψ cross section scaled by the branching ratio B as a function of p_T in the di-muon decay channel (black circle) and in the di-electron decay channel (red circle).

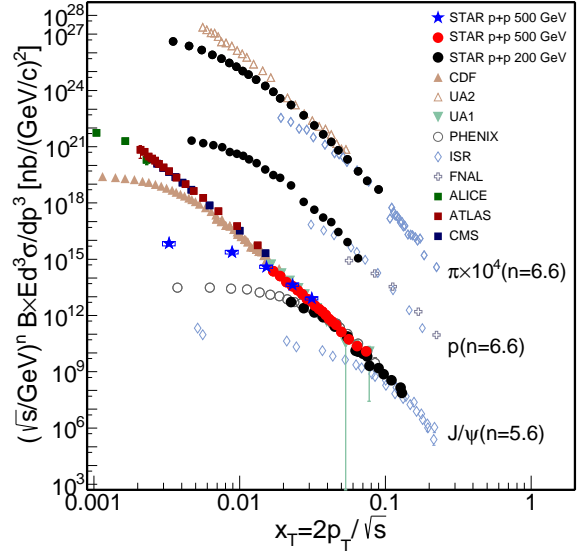


Figure 2. x_T scaling of J/ψ cross section scaled by the branching ratio B in the di-muon decay channel (blue star) and in the di-electron decay channel (red circle).

2. J/ψ measurements in p+p collisions at $\sqrt{s} = 500$ GeV

Figure 1 shows the cross section of J/ψ in p+p collisions at $\sqrt{s} = 500$ GeV in the di-electron and di-muon decay channels for $0 < p_T < 20$ GeV/c. The di-muon decay channel extends p_T reach down to 0 GeV/c. The results in these decay channels are consistent in the overlapping p_T range of $4 < p_T < 9$ GeV/c. The experimental results can be well described by CGC+NRQCD calculations at low p_T [4] and NLO NRQCD calculations at high p_T [5]. Figure 2 shows the $x_T = 2p_T/\sqrt{s}$ scaling of J/ψ cross section [6]. The J/ψ cross section in p+p collisions at $\sqrt{s} = 500$ GeV follows the common trend as a function of x_T at high p_T . The breaking of the x_T scaling at low p_T can be attributed to the soft processes.

3. J/ψ measurements in Au+Au collisions at $\sqrt{s_{NN}} = 200$ GeV

Figure 3 shows the invariant yield of J/ψ in Au+Au collisions at $\sqrt{s_{NN}} = 200$ GeV for different collision centralities. The new results in the di-muon decay channel are consistent with previous results in the di-electron decay channel [7, 8] within uncertainties.

The nuclear modification factor $R_{AA} = \frac{\sigma_{inel}}{\langle N_{coll} \rangle} \frac{d^2 N_{AA}/dy dp_T}{d^2 \sigma_{pp}/dy dp_T}$ of J/ψ in 0-40% central Au+Au collisions is shown in Fig. 4, compared with LHC results [13, 14]. The strong suppression at RHIC at low p_T indicates that dissociation plays a significant role in this p_T range. The hint of the increasing trend of R_{AA} at RHIC at high p_T can be explained by formation-time effects and feed-down of B hadrons. The less suppression of J/ψ at LHC at low p_T indicates larger regeneration contribution due to higher charm cross section, while more suppression of J/ψ at LHC at high p_T indicates larger dissociation rate due to higher temperature of the medium. Transport Models from Tsinghua [9, 10] and Texas A&M University (TAMU) [11, 12], including dissociation and regeneration effects, can qualitatively describe the p_T dependence of RHIC and LHC data.

Centrality dependence of J/ψ cross section is shown in Fig. 5 for integrated p_T and in Fig. 6 for $p_T > 5$ GeV/c. For integrated p_T , both models can describe centrality dependence at RHIC, but tend to overestimate suppression at LHC. For $p_T > 5$ GeV/c, there is tension among models

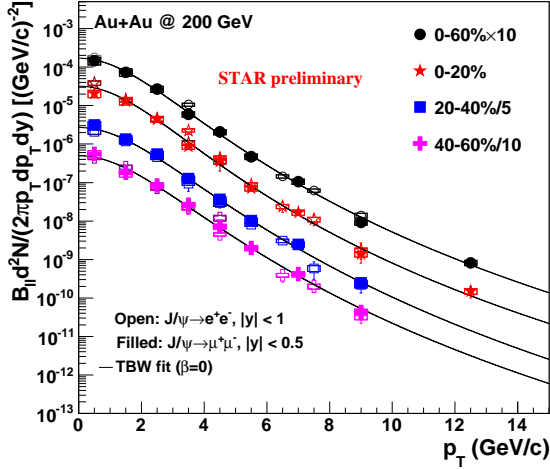


Figure 3. Invariant yield of J/ψ scaled by the branching ratio B_{ll} as a function of p_T in different centralities in the di-muon decay channel (filled) and in the di-electron decay channel (open).

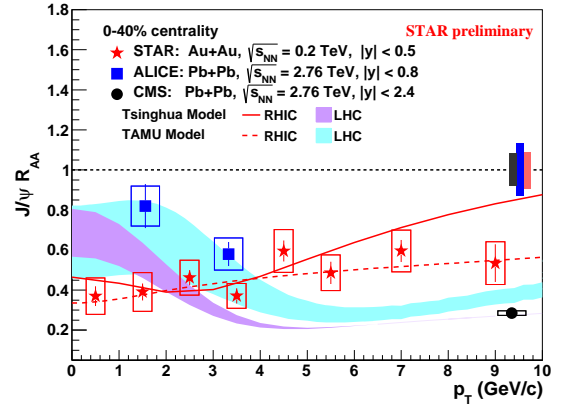


Figure 4. R_{AA} as a function of p_T at RHIC (red star) and at LHC (blue square, black circle). The lines and bands indicate Transport Model calculations for RHIC and LHC energies.

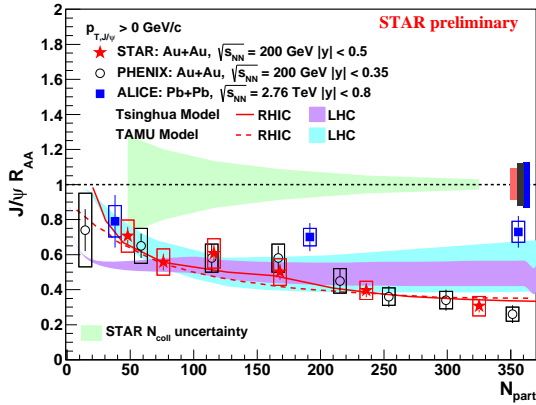


Figure 5. Nuclear modification factor R_{AA} for integrated p_T as a function of N_{part} .

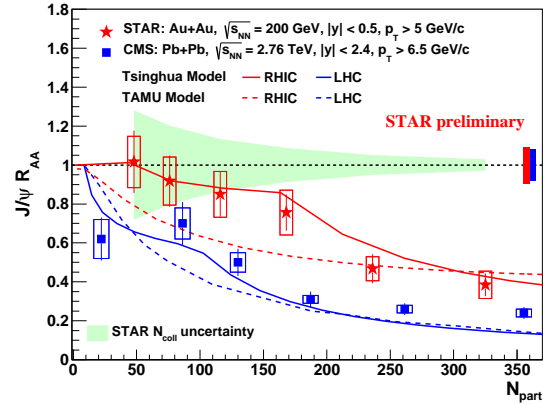


Figure 6. Nuclear modification factor R_{AA} for $p_T > 5$ GeV/c as a function of N_{part} .

and data. New measurements in the di-muon decay channel provide a distinguishing power for these transport models.

4. Υ measurements in Au+Au collisions at $\sqrt{s_{NN}} = 200$ GeV

Figure 7 shows the di-muon mass spectrum in Υ state mass range in Au+Au collisions at $\sqrt{s_{NN}} = 200$ GeV. We observe signs of an indication of $\Upsilon(2S + 3S)$ signals in the di-muon decay channel. The raw yields of Υ states are obtained by a simultaneous fit to the like-sign and unlike-sign distributions. In this fit, (i) the Υ state masses are fixed to the PDG values and their widths are determined by simulation; (ii) the ratio of $\Upsilon(2S)/\Upsilon(3S)$ is fixed to the value in p+p collisions; and (iii) the shape of $b\bar{b}$ and Drell-Yan background is estimated using PYTHIA. Figure 8 shows the fitted $\Upsilon(2S + 3S)/\Upsilon(1S)$ ratio compared with the world-wide p+p data [16] and CMS data [17, 18]. There is a hint of less melting of $\Upsilon(2S + 3S)$ relative to $\Upsilon(1S)$ at RHIC

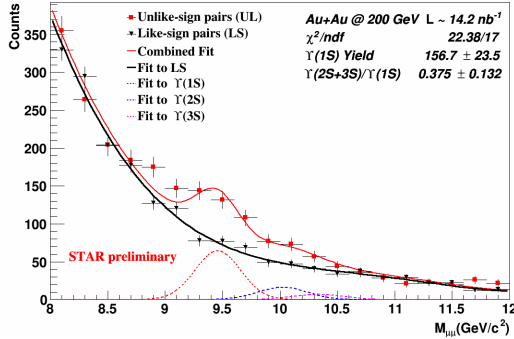


Figure 7. Di-muon mass spectrum in the Υ state mass range.

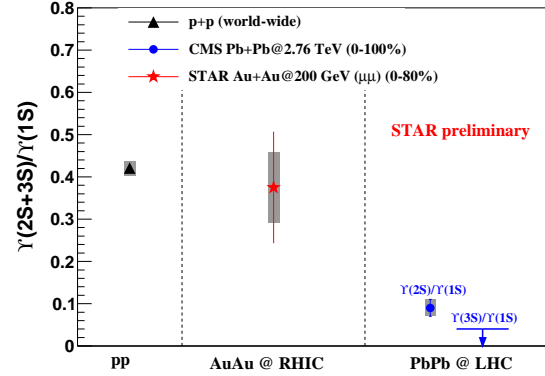


Figure 8. $\Upsilon(2S+3S)/\Upsilon(1S)$ ratio for world-wide p+p data, and for heavy-ion collisions at RHIC, and LHC energies.

than at LHC.

5. Summary and Outlook

We present the first J/ψ and Υ measurements in the di-muon decay channel at mid-rapidity at RHIC. In p+p collisions at $\sqrt{s} = 500$ GeV, inclusive J/ψ cross section can be described by CGC+NRQCD and NLO NRQCD model calculations for $0 < p_T < 20$ GeV/c. In Au+Au collisions at $\sqrt{s_{NN}} = 200$ GeV, we observe (i) clear J/ψ suppression indicating dissociation; (ii) $J/\psi R_{AA}$ can be qualitatively described by transport models including dissociation and regeneration despite a tension at high p_T ; and (iii) there is a hint of less melting of $\Upsilon(2S + 3S)$ relative to $\Upsilon(1S)$ at RHIC compared to that at LHC. These measurements in Au+Au collisions will have better statistical precision by combining the similar amount of data recorded in the RHIC 2016 run.

References

- [1] T. Matsui and H. Satz, *Phys. Lett. B* **178** 416-422 (1986)
- [2] A. Adare *et. al.* (PHENIX Collaboration), *Phys. Rev. Lett.* **103** 082002 (2009)
- [3] L. Adamczyk *et. al.* (STAR Collaboration), *Phys. Rev. D* **86** 072013 (2012)
- [4] Yan-Qing Ma and Raju Venugopalan, *Phys. Rev. Lett.* **113** 192301 (2015)
- [5] H. Shao *et. al.*, *JHEP* **05** 103 (2015)
- [6] B. Abelev *et. al.* (STAR Collaboration), *Phys. Rev. C* **80** 041902 (2009)
- [7] L. Adamczyk *et. al.* (STAR Collaboration), *Phys. Let. B* **722** 55-62 (2013)
- [8] L. Adamczyk *et. al.* (STAR Collaboration), *Phys. Rev. C* **90** 024906 (2014)
- [9] Y. Liu *et. al.*, *Phys. Let. B* **678** 72-76 (2009)
- [10] K. Zhou *et. al.*, *Phys. Rev. C* **89** 054911 (2014)
- [11] X. Zhao and R. Rapp, *Phys. Rev. C* **82** 064905 (2010)
- [12] X. Zhao and R. Rapp, *Nucl. Phys. A* **859** 114-125 (2011)
- [13] B. Abelev *et. al.* (ALICE Collaboration), *Phys. Let. B* **734** 314-327 (2014)
- [14] S. Chatrchyan *et. al.* (CMS Collaboration), *JHEP* **05** 063 (2012)
- [15] L. Adamczyk *et. al.* (STAR Collaboration), *Phys. Rev. Lett.* **111** 052301 (2013)
- [16] W. Zha *et. al.*, *Phys. Rev. C* **88** 067901 (2013)
- [17] S. Chatrchyan *et. al.* (CMS Collaboration), *Phys. Rev. Lett.* **109** 222301 (2012)
- [18] S. Chatrchyan *et. al.* (CMS Collaboration), *JHEP* **04** 103 (2014)